Cellular/Molecular

Acetaldehyde Excitation of Lateral Habenular Neurons via Multiple Cellular Mechanisms

Weiyuan Huang,[1,2*] Wanhong Zuo,[1*] Lixin Chen,[2] Liwei Wang,[2] George Tewfik,[1] Rao Fu,[1] Jiayi Zheng,[1] Ding Li,[1] and Jiang-Hong Ye[1]

[1]Department of Anesthesiology, Pharmacology and Physiology, & Neuroscience Rutgers, The State University of New Jersey, New Jersey Medical School, Newark, New Jersey, 07103, and [2]Department of Physiology, and Pharmacology, Medical College, Jinan University, Guangzhou, 510632 China

Acetaldehyde (ACD), the first metabolite of ethanol, is implicated in several of ethanol's actions, including the reinforcing and aversive effects. The neuronal mechanisms underlying ACD's aversive effect, however, are poorly understood. The lateral habenula (LHb), a regulator of midbrain monoaminergic centers, is activated by negative valence events. Although the LHb has been linked to the aversive responses of several abused drugs, including ethanol, little is known about ACD. We, therefore, assessed ACD's action on LHb neurons in rats. The results showed that intraperitoneal injection of ACD increased cFos protein expression within the LHb and that intra-LHb infusion of ACD induced conditioned place aversion in male rats. Furthermore, electrophysiological recording in brain slices of male and female rats showed that bath application of ACD facilitated spontaneous firing and glutamatergic transmission. This effect of ACD was potentiated by an aldehyde dehydrogenase (ALDH) inhibitor, disulfiram (DS), but attenuated by the antagonists of dopamine (DA) receptor (DAR) subtype 1 (SCH23390) and subtype 2 (raclopride), and partly abolished by the pretreatment of DA or DA reuptake blocker (GBR12935; GBR). Moreover, application of ACD initiated a depolarizing inward current (I_{ACD}) and enhanced the hyperpolarizing-activated currents in LHb neurons. Bath application of Rp-cAMPs, a selective cAMP-PKA inhibitor, attenuated ACD-induced potentiation of EPSCs and I_{ACD}. Finally, bath application of ZD7288, a selective blocker of hyperpolarization-activated cyclic nucleotide-gated channels, attenuated ACD-induced potentiation of firing, EPSCs, and I_{ACD}. These results show that ACD exerts its aversive property by exciting LHb neurons via multiple cellular mechanisms, and new treatments targeting the LHb may be beneficial for alcoholism.

Key words: **aversion; cAMP-PKA; dopamine receptor; electrophysiology; HCN channels; immunochemistry**

Significance Statement

Acetaldehyde (ACD) has been considered aversive peripherally and rewarding centrally. However, whether ACD has a central aversive property is unclear. Here, we report that ACD excites the lateral habenula (LHb), a brain region associated with aversion and negative valence, through multiple cellular and molecular mechanisms. Intra-LHb ACD produces significant conditioned place aversion. These results suggest that ACD's actions on the LHb neurons might contribute to its central aversive property and new treatments targeting the LHb may be beneficial for alcoholism.

Introduction

Ethanol, like many other abused drugs, has rewarding and aversive properties, both of which contribute to the development of alcohol use disorders (Barkley-Levenson et al., 2015). While it is well documented that ethanol's rewarding property is associated with its ability to activate the mesolimbic dopaminergic system, we know much less about its aversive property. Ethanol is metabolized through a complex catabolic metabolic pathway. Several enzymes are involved in processing ethanol first into acetaldehyde (ACD) and further into acetic acid. Ethanol is oxidized to ACD, mainly via the enzyme alcohol dehydrogenase (ADH). The enzyme associated with the chemical transformation from ACD to acetic acid is aldehyde dehydrogenase (ALDH).

ACD is a highly unstable compound and quickly forms free radical structures which are highly toxic. ACD has long been recognized as a major aversive compound (Hunt, 1996), although recent evidence indicates that it is also involved in various neuropharmacological, neurobiological, and behavioral effects of ethanol; ACD in the brain may also contribute to ethanol's

Received Nov. 16, 2020; revised June 26, 2021; accepted July 25, 2021.

Author contributions: J.-H.Y., W.H., and W.Z. designed research; W.H., W.Z., R.F., D.L., and J.Z. performed research; J.-H.Y., W.H., W.Z., D.L., and J.Z. analyzed data; W.H. wrote the first draft of the paper; J.-H.Y., W.Z., L.C., L.W., and G.T. edited the paper; J.-H.Y. wrote the paper.

This work is supported by National Institutes of Health National Institute on Alcohol Abuse and Alcoholism Grants AA021657 and AA022292 (to J.-H.Y.).

*W.H. and W.Z. contributed equally to this work.

The authors declare no competing financial interests.

Correspondence should be addressed to Jiang-Hong Ye at ye@njms.rutgers.edu.

https://doi.org/10.1523/JNEUROSCI.2913-20.2021

motivational property (Peana et al., 2017). However, the neurobiological mechanism underlying ACD's effects, the aversive effect in particular, has not been well elucidated.

Accumulating evidence shows that the lateral habenula (LHb), a hub-like epithalamus structure in the brain, is a crucial negative regulator of midbrain monoaminergic systems (Hu et al., 2020). Activation of the LHb can inhibit midbrain dopamine (DA) neuron firing (Ji and Shepard, 2007; Matsumoto and Hikosaka, 2007). The LHb is involved in the control of motivated behavior via signaling in the absence of a predicted reward, and information regarding aversive stimuli to brain reward areas (Matsumoto and Hikosaka, 2007, 2009; Jhou et al., 2009; Bromberg-Martin and Hikosaka, 2011). The LHb conveys negative reward signals to midbrain DA neurons and plays a crucial role in drugs of abuse (Mathis and Kenny, 2019), including nicotine (Khaled et al., 2014), cocaine (Meye et al., 2016), heroin (Zhang et al., 2005), morphine (Valentinova et al., 2019), amphetamine (Gifuni et al., 2012), and ethanol (Li et al., 2016, 2017, 2019; Kang et al., 2017; Sheth et al., 2017; Fu et al., 2021). However, the effects of ACD on the LHb have not been investigated.

In this study, to test the hypothesis that ACD's activation of LHb contributes to its central aversive properties, we examined the effects of systemic administration of ACD on cFos expression in the LHb of rats. We then determined the effect of intra-LHb infusion of ACD on place conditioning preference. Moreover, using electrophysiological recording in brain slices, we examined the effects of ACD on the neuronal activity, the glutamatergic transmission, membrane currents, and hyperpolarization-activated currents (I_h) of LHb neurons. We additionally examined the roles of dopaminergic signaling, of the cAMP-PKA and HCN channels in the effects of ACD.

Materials and Methods

Animals

All procedures were performed by the National Institutes of Health guidelines and with the approval of the Animal Care and Utilization Committee of Rutgers, the State University of New Jersey, by the guidelines of the National Institutes of Health (*Guide for the Care and Use of Laboratory Animals*), minimizing the number of animals and their suffering. Experiments were done on Sprague Dawley rats (Envigo). The rats were housed with a standard 12/12 h light/dark cycle with *ad libitum* food and water. We performed c-Fos immunohistochemistry and place conditioning in male rats [postnatal day (PND)60–PND70, $n = 30$], and electrophysiological recordings from both juvenile (PND17–PND25, $n = 120$) and adult (PND60–PND90, $n = 40$) rats of both sexes.

Slice preparation and electrophysiological recording

Rats were anesthetized with ketamine/xylazine (80/10 mg/kg, i.p.) and killed. Brains were rapidly removed and placed in a beaker containing ice-cold carbogenated (95% O_2/5% CO_2) artificial CSF (aCSF) containing the following: 126 mM NaCl, 2.5 mM KCl, 1.25 mM NaH_2PO_4, 1 mM $MgCl_2$, 2 mM $CaCl_2$, 25 mM $NaHCO_3$, 1 mM L-ascorbate, and 11 mM glucose. The brain was then trimmed with a razor blade, and a block of tissue containing the LHb was glued onto the cutting stage of Compresstome VF-200 slicer (Precisionary Instruments Inc.). Coronal epithalamic slices (250 μM) were prepared in carbogenated, ice-cold glycerol-based aCSF containing almost the same components as regular aCSF except for replacing NaCl with 251 mM glycerol (Ye et al., 2006). Slices were then incubated for at least 30 min in warm (35°C) carbogenated aCSF, before being transferred to the recording chamber that was constantly perfused with carbogenated aCSF at the rate of 2 ml/min at 33°C maintained by an automatic temperature controller (Warner Instruments).

LHb neurons were visualized with a 40× water-immersion objective on an upright microscope (Nikon Eclipse, E600FN) and near-infrared illumination. The electrophysiological recording was performed using an Axon 700A amplifier, a Digidata 1322A analog-to-digital converter, and pClamp 10.4 software (Molecular Devices Co). Patch pipettes had a resistance of 5–8 MΩ when filled with a solution containing the following: 140 mM cesium methanesulfonate, 5 mM KCl, 2 mM $MgCl_2$, 10 mM HEPES, 2 mM MgATP, 0.2 mM GTP for voltage-clamp recordings or 140 mM K-gluconate, 5 mM KCl, 2 mM $MgCl_2$, 10 mM HEPES, 2 mM MgATP, and 0.2 mM GTP for current-clamp and h current (I_h) recording (pH 7.2, with Tris-base; 310 mOsmol/l, with sucrose). The spontaneous firing activity was recorded under loose seal cell-attached voltage-clamp mode ($V = 0$) or whole cell current-clamp mode ($I = 0$). Both evoked EPSCs (eEPSCs) and spontaneous EPSCs (sEPSCs), mediated by AMPA receptors, were recorded at a holding potential (V_H) of −60 mV in the presence of gabazine (10 μM) and strychnine (1 μM) to block $GABA_A$ and glycine receptors, respectively. Paired evoked postsynaptic currents were recorded using a nichrome wire bipolar stimulating electrode which was positioned within 200 μm of the soma. A pair of identical electrical stimuli (100–200 μs in duration) separated by an interval of 50 ms was given at the rate of 0.05 Hz. The stimulating intensity was set to 20–30% of the maximum and the input/output curve was recorded when the response was stable with no failures. The ACD-induced inward current was recorded at a V_H of −60 mV in the presence of tetrodotoxin (TTX; 0.5 μM), 6,7-dinitroquinoxaline-2,3-dione (DNQX; 20 μM), DL-2-amino-5-phosphono-valeric acid (DL-AP5; 50 μM), gabazine (10 μM), and strychnine (1 μM). Whole-cell voltage clamp was used to record I_h with a series of 1.5-s pulses with a 10-mV command voltage step from −120 to −60 mV from a V_H of −60 mV. The peak instantaneous current was measured at the first 50 ms of the beginning of each 1.5-s hyperpolarizing voltage command step of each sweep and the steady-state current was measured as the average value from the last 50 ms at the end of each 1.5-s hyperpolarizing voltage. The amplitude of I_h was measured by deducting instantaneous current from steady-state current at each sweep. I_h positive (I_h^+) neurons were defined as having an I_h (peak to steady state trough) > 10 pA (and conversely I_h^- neurons have an $I_h \leq 10$ pA).

Peak I_h was fitted with a Boltzmann equation: $I_h/I_{max} = [1+exp(V - V_{1/2})]/k$, where I_{max} is the maximal I_h, $V_{1/2}$ is the half-activation potential, and k is the slope factor. I_{max} was normalized to the largest current of the control group.

Implantation of cannulae

Stereotaxic surgery and histologic verification were performed on adult rats as previously described (Zuo et al., 2017, 2019). Bilateral guide cannulae (FIT 5MM C232G-1.5W-1MM PROJ, 28 gauge; Plastics One) were inserted dorsally to the LHb (−3.8 AP, ±0.75 ML, −4.2 DV).

Intra-LHb microinjections of chemicals

The experiments were conducted as previously described (Zuo et al., 2017). Briefly, aCSF (vehicle, 500 nl/side) or ACD (diluted in aCSF, 90 μM/500 nl/side, as described prevously; Rodd-Henricks et al., 2002; Deehan et al., 2013b) was administered into the LHb. The injector extended 1.0 mm beyond the guide cannulae tip, infusion lasted for 60 s, and injectors were left in place for an additional 60 s to allow for diffusion and to prevent diffusion up the cannula.

Conditioning place preference (CPP) experiments apparatus

The CPP experiment was conducted as previously described (Zuo et al., 2017). Briefly, the CPP box was divided by a guillotine door into two distinct compartments of equal size (44.4 L × 44.4 W × 30.5 H, in cm; Med Associates Inc), but with different floor textures patterns: one with a grid floor, the other with a wire mesh floor. The chambers were illuminated by a 40-W light. Time spent in each chamber was measured during each phase of the CPP using video tracking followed by the analysis by Smart 3.0 (Panlab Harvard Apparatus).

Experimental procedure and treatment

Rats were allowed to recover from surgery for 14 d before place conditioning tests (Fig. 1*D*). During this period, rats were brought to the experimental room and handled for 5 min each day. The place

conditioning procedure consisted of three phases: pretest (day 25), conditioning (days 26–28), and post-test (day 29).

Preconditioning test

On day 25, each animal was placed in one of the two compartments in a counter balanced manner and allowed to explore both environments for 15 min. Time spent in each compartment was automatically measured by a PC software and initial preference or aversion for one side of the two compartments was determined. Rat that spent >70% of the time in any of the two chambers were excluded from further evaluation. In the current study, most rats spent roughly equal time in the two compartments (wire mesh = 442.1 ± 8.7 s, grid = 456.7 ± 8.7 s, $n = 28$, $p = 0.41$), indicating no unconditioned baseline preference for either chamber, supporting the unbiased method.

Conditioning

During the 3 d of conditioning (days 25–28), 28 animals were divided into two groups and intra-LHb microinjected twice a day with either aCSF or ACD. After receiving microinjection, rats were returned to home cages for 5 min before being confined in the assigned compartments (wire mesh or grid, randomly chosen) for 15 min. aCSF group was paired with receiving aCSF in both sides of boxes, while the ACD group with receiving aCSF (morning, starting at 8 A.M.) on one of the sides and ACD (afternoon, starting at 3 P.M.) on the opposite side. The connecting area was not accessible during conditioning and was blocked by guillotine doors.

Postconditioning test

On day 29, 20 h following the last conditioning session, animals were tested in a drug-free state. Rats explored the compartments for 15 min with guillotine doors opened and time spent in each compartment was recorded for each animal. The preference score was calculated for each rat by the difference in times spent in the ACD-paired and aCSF-paired chambers on the post-testing day compared with the pretest day. Positive or negative scores indicated preference or aversion, respectively.

Immunohistochemistry

Male rats were divided into three groups ($n = 4$/group): saline, ACD, 100 mg/kg, and 300 mg/kg. These two doses (100 and 300 mg/kg) were chosen because it has been shown that ACD at these doses induces CTA in rats (Aragon et al., 1991; Quintanilla and Tampier, 2003). A previous rodent study found that intraperitoneal administration of ACD (100 mg/kg) raised brain ACD level at ~100 μM within 5 min and remained at μM levels for 30 min (Jamal et al., 2016). In current study, 1 h after systemic administration of saline or ACD, the rats were deeply anesthetized with ketamine/xylazine (80/10 mg/kg, i.p.) and transcardially perfused with cold saline followed by 4% paraformaldehyde in 0.1 M sodium phosphate buffer (pH 7.4). After that, brains were removed and post-fixed (2 h, at 4°C) in the fixative solution and then cryoprotected in 20% sucrose in 0.1 M phosphate buffer (4°C, pH 7.4). Serial coronal sections (30 μm) that included the LHb were cut on a freezing microtome (Microm HM550) and then processed for immunohistochemical detection of cFos protein. The sections were treated with 0.3% hydrogen peroxide solution and then incubated in a solution containing 0.3% Triton X-100 (v/v) and 3% normal goat serum for 30 min. Next, the brain sections were incubated with anti-cFos rabbit polyclonal antibodies (1:15,000 in 0.1 M PBS containing 3% normal goat serum and 0.2% Triton X-100; EMD Chemicals Inc.) overnight at 4°C. After several rinses with PBS, sections were placed in a solution of biotinylated goat-anti-rabbit antibody (1:200, Vector Laboratories) for 2 h. Sections were washed several times in PBS and then treated with avidin-biotin-peroxidase complex (1:400, Vectastain ABC Elite, Vector Laboratories) and visualized with nickel-intensified diaminobenzidine [0.02% (w/v) 3,30-diaminobenzidine, 2.5% (w/v) nickel ammonium sulfate and 0.000083% (v/v) H_2O_2, in 0.175 M sodium acetate].

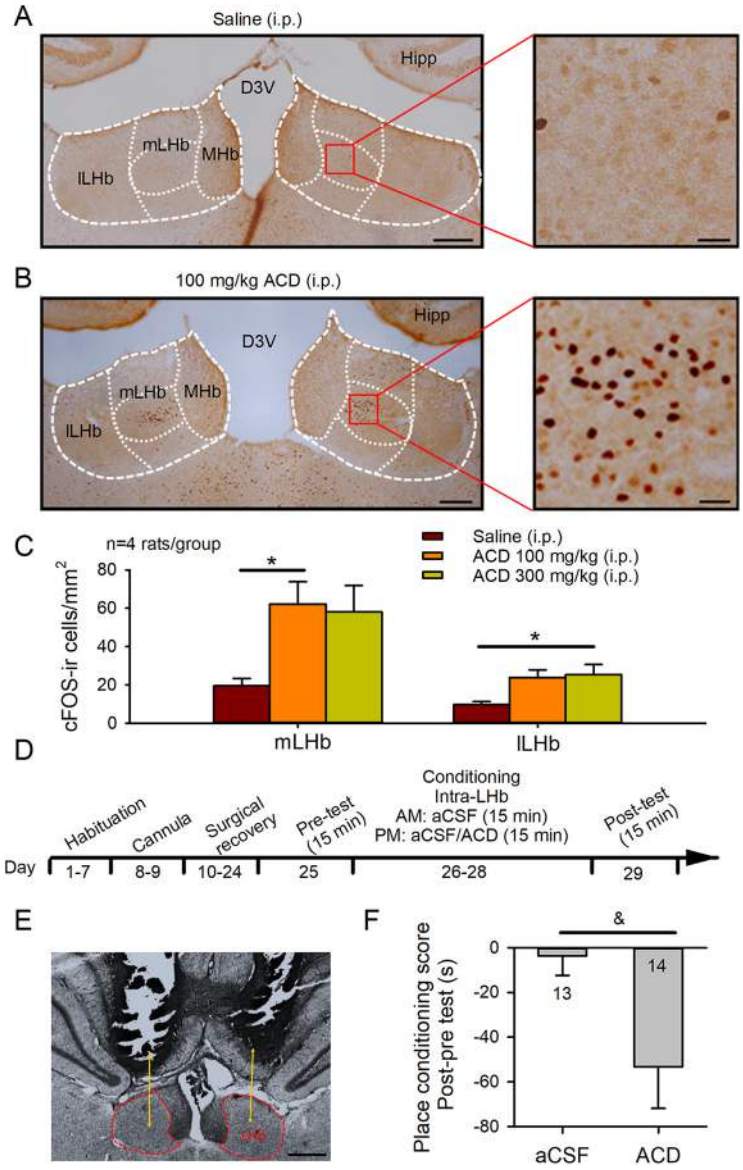

Figure 1. ACD administration activates lateral habenula neurons and induces conditioned place aversion. Systemic administration (intraperitoneal injection) of ACD robustly increases immunoreactive cFos expression in the habenula of Sprague Dawley rats. Low-magnification (4×) and high-magnification (20×) images of habenula showing that ACD increases cFos expression in coronal sections of brain slices which were obtained 1 h after injection of saline (***A***) or ACD (100 mg/kg, ***B***). Hipp, Hippocampus; D3V, third ventricle; MHb, medial habenula; mLHb, medial part of LHb; lLHb, lateral part of LHb. Scale bars: 200 and 25 μm, respectively, for the left and the right panels. ***C***, Mean number (±SEM) of cFos-IR cells per mm^2 in the mLHb and lLHb after injection of saline, 100 mg or 300 mg/kg ACD; *$p < 0.05$ ACD versus saline, one-way ANOVA. ***D***, Experimental timeline of cannula surgeries and conditioning place testing schedule. ***E***, Cannula injection sites. Scale bar: 500 μm. ***F***, In the place conditioning paradigm, intra-LHb infusion of ACD significantly decreased the place conditioning score. Numbers of rats were indicated; &$p < 0.05$ aCSF versus ACD, Student's unpaired t test (two-tailed).

The cFos immunoreactive cells were counted stereologically in the entire LHb, the blinded analysis was performed in a 30-μm section every 120 μm using an assisted image analysis system, a Nikon DS-Ril digital camera, Nikon Eclipse 8oi microscope at 4× or 20× magnification and analyzed with NIS-Elements BR 3.0 software (Micron Optics, Nikon).

Chemicals

All chemicals including ACD, cadmium chloride ($CdCl_2$), DNQX, AP5, SCH23390, raclopride, gabazine, Rp-cAMPs, (9S,10S,12R)−2,3,9,10,11,12-hexahydro-10-hydroxy-9-methyl-1-oxo-9,12-epoxy-1H-diindolo [1,2,3-fg: 3',2',1'-kl] pyrrolo[3,4-i] [1,6] benzodiazocine-10-carboxylic acid hexyl ester (KT-5720), strychnine, ZD7288, disulfiram (DS), DA, GBR12935 (GBR), TTX, 4-methylpyrazole (4-MP), and acetate were purchased from Sigma. Drugs were diluted immediately before used into the final concentration with saline, aCSF, or pipette solution wherever proper.

Data analysis and statistics

All data were expressed as mean ± SEM. Electrophysiological data from both the males and the females were not significantly different and therefore were pooled. Data analysis was conducted as previously described (Zuo et al., 2017). Briefly, baseline electrophysiological data were recorded for 5–10 min, before drug superfusion, and during the washout. Since the basal firing rate and EPSC frequency and amplitude vary in each cell, changes induced by each drug were calculated by the percent change. Data recorded during the initial control period were averaged and normalized to 100%. Before analysis, the distributions of the variables under study were examined using histograms. The use of parametric statistical analysis was deemed appropriate.

Percent change of EPSC or firing frequency for a given cell was calculated, the recordings during the 3- to 5-min baseline before ACD (or other chemical) application were averaged and normalized to 100%. Each chemical was perfused for 8–10 min, the data in the last 3 min were analyzed and compared with the baseline. Statistical analysis was performed using a two-tailed Student's *t* test, a one-way ANOVA with a Tukey's *post hoc* test for multiple group comparisons unless otherwise noted. The Kolmogorov–Smirnov (K-S) test was used to analyze differences in the average cumulative probability distributions. Dose–response data were fit to the logistic equation:$y = 100\,x^a/(x^a + x_0^a)$, where y is the percentage change, x is the concentration of ACD, a is the slope parameter, and x_0 is the ACD concentration which induces a half-maximal change. Significance for all analyses was determined at $p < 0.05$.

Results

Systemic administration of ACD increases cFos expression in a subpopulation of LHb neurons

To determine whether ACD might activate LHb neurons, we first examined cFos expression. A dense cluster of cFos immunoreactive cells was found within the medial (mLHb; $F_{(2,9)} = 4.83$, $p = 0.038$) and lateral (lLHb; $F_{(2,9)} = 4.79$, $p = 0.038$) aspects of the LHb in rats injected with ACD (intraperitoneally), but not with saline (*post hoc* $p < 0.05$; Fig. 1*A*–*C*). No significant difference in the effect on cFos expression was found between 100 and 300 mg/kg of ACD ($p > 0.5$; Fig. 1*C*).

Intra-LHb injection of ACD elicits a significant place aversion

Histologic analysis revealed that the injector tracks in the 28 animals, except one, terminated at a point within the habenula (Fig. 1*D*,*E*). Thus, the data of the one outside the LHb was excluded. As expected, animals injected with aCSF and paired in both chambers, showed no preference for either chamber. Conversely, the ACD-treated rats spent significantly shorter time in ACD-paired compartment after three conditioning trials compared with aCSF controls ($t_{(25)} = 2.3$, $p = 0.027$; Fig. 1*F*).

ACD stimulates a subpopulation of mLHb neurons

To determine the mechanisms by which ACD activates LHb neurons, we assessed the effect of ACD on the spontaneous firing of mLHb neurons from both the juvenile and the adult rats. Firing changes recorded in cell-attached or whole-cell current-clamp modes were not significantly different, and thus were pooled. A previous mouse study showed that the effect of ACD depends on its dose, and that blood and brain ACD concentration reached a sharp peak at 5 min and then quickly declined for 60 min after systemic ACD administration. After ACD (100 mg/kg, i.p.), ACD concentrations in the brain was ~100 μM, which was close to those in the blood (130 μM; Jamal et al., 2016). Based on this information, we tested the effects of ACD (0.1–100 μM) in the brain slices. We recorded 589 neurons in mLHb of 120 juvenile rats. Among them, 227(38.9%) neurons fired tonically, 120 (21.2%) cells fired in burst, and the rest 240 (40.7%) were silent. Eight silent neurons from seven rats kept silent after 5 min bath perfusion of ACD (10.0 μM). In nine bursting neurons from seven rats, ACD (10 μM) did not change the activity of six neurons, while gradually turned into tonic firing pattern in the other three neurons (data not shown). ACD significantly changed the activity of tonically fired neurons. We thus focused on the tonic firing cells.

In the juvenile rats ($n_{rats} = 80$), bath perfusion of ACD (0.1–50 μM) significantly increased the firing rate in the mLHb neurons ($F_{(5,35)} = 12.8$, $p < 0.001$; Fig. 2*A*,*B*). Specifically, 10 μM ACD accelerated the firing rate by 58.5 ± 11.1% ($n = 10$, *post hoc* $p < 0.01$ vs aCSF). The firing returned to the control levels on washout of ACD. In a subgroup of neurons, repeated application of ACD to the same neuron after washout produced an acceleration that was not significantly different from the first one ($p > 0.5$; Fig. 2*B*,*C*). ACD also increased the firings of mLHb neurons ($F_{(4,53)} = 48.7$, $p < 0.001$) of the adult rats ($n_{rats} = 40$). The effect of ACD depends on its concentrations in LHb neurons of both juvenile and adult rats. The concentration-response curves are well fit by the logistic equation, with an apparent EC_{50} of 8.0 μM ($r^2 = 0.99$; Fig. 2*D*) in the juvenile rats and of 3.2 μM ($r^2 = 0.95$; Fig. 2*D*) in the adult rats, respectively. To determine how the ACD-sensitive mLHb neurons respond to ethanol, we applied ethanol to the same neurons after washout of ACD. Bath application of ethanol (21 mM) caused a robust acceleration of firing of mLHb neurons of juvenile rats as those produced by 10 μM ACD ($n_{cells} = 9$ from 8 rats; Fig. 2*E*).

To determine whether ACD is involved in the excitation induced by ethanol, brain slices were incubated for 30 min in 4-MP (0.5 mM), an ADH inhibitor, before the electrophysiological recording. Ethanol-induced enhancement of firing was significantly decreased after pretreating the LHb neurons with 4-MP ($t_{(19)} = 2.8$, $p = 0.012$, EtOH vs 4-MP+EtOH; Fig. 2*F*), indicating that ethanol's acute effect on mLHb firing depends, at least in part, on its first metabolite ACD. We further assessed the effect of ethanol metabolites by examining the effect of acetate. Bath perfusion of acetate (1 mM) significantly reduced the spontaneous firing rate by 50.1 ± 10.7% ($t_{(9)} = 3.24$, $p = 0.01$ vs baseline; Fig. 2*F*), indicating that acetate is not responsible for the excitation of mLHb neurons by ethanol and ACD.

A previous histochemical study found ALDH activity in the cytoplasm and in the terminal regions of neurons, as well as glial cells, and moderate ALDH activity in the LHb (Zimatkin, 1991). To determine whether ALDH activity functionally affects LHb neurons, we applied DS (10 μM), an ALDH inhibitor to the brain slices. Interestingly, DS significantly increased the firing rate of mLHb neurons ($t_{(11)} = 3.0$, $p = 0.011$), suggesting the existence of

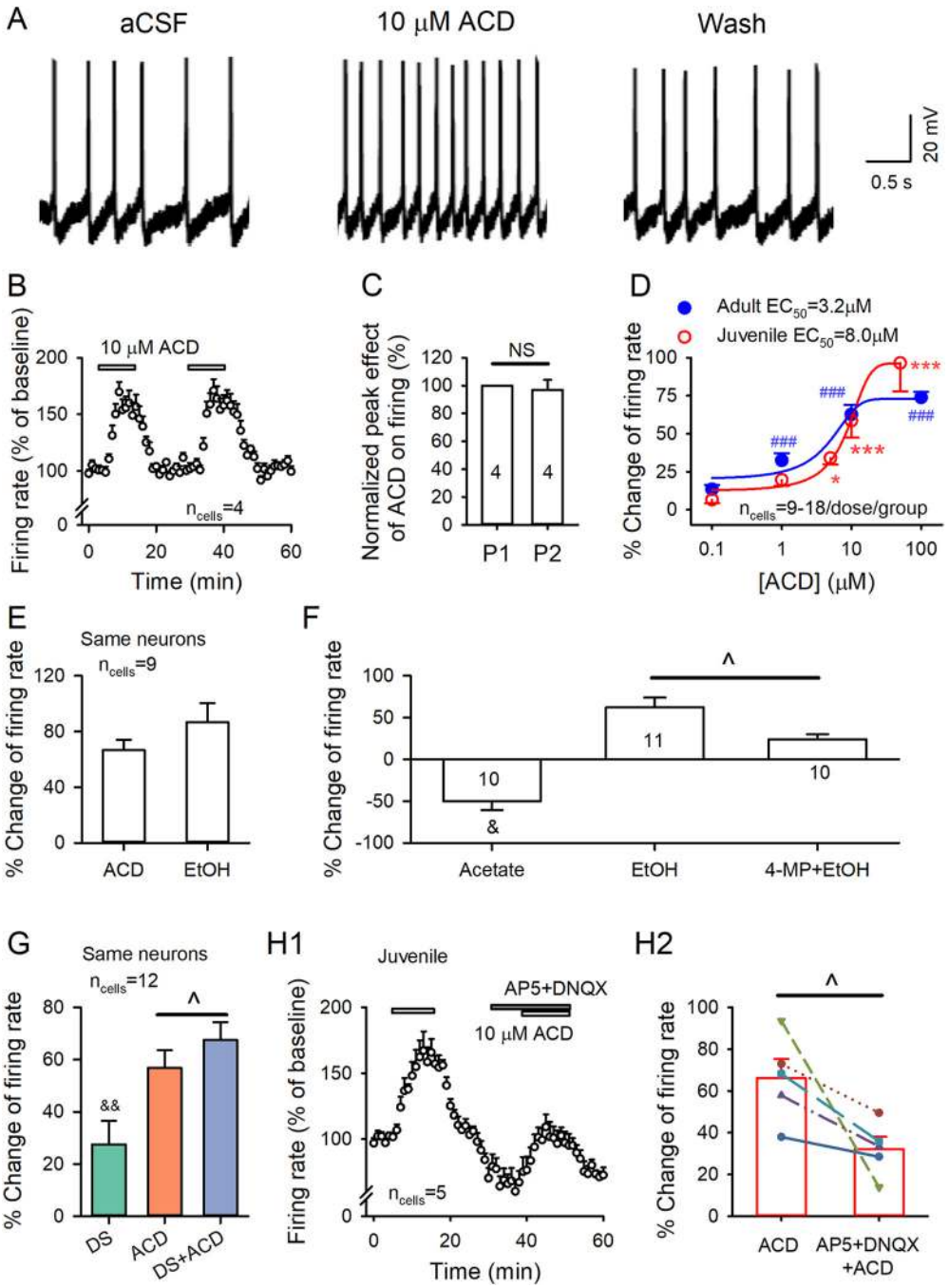

Figure 2. ACD accelerates mLHb neuron firing, which is partly mediated by the glutamate receptors. ***A***, Voltage traces show ACD (10 μM) accelerated the spontaneous firings of an mLHb neuron. ***B***, Mean of the time course of ACD-induced facilitation of firing of an mLHb neuron. For this and the other figures, the horizontal bar above the time course histogram signals the application of the indicated drug. ***C***, Repeated application of ACD induced a similar increase in mLHb neurons firing rate. The numbers of cells are indicated. ***D***, The concentration-response relationship of ACD-induced acceleration of firing rate in mLHb neurons. For all figures, circles and error bars are mean and SEM, respectively. The smooth curve is the best fit of the data to the logistic equation; $^{*}p < 0.01$, $^{***}p < 0.001$(juvenile); $^{\#\#\#}p < 0.001$ (adult); one-way ANOVA followed by Tukey's multiple comparisons test. ACD application versus aCSF (ACD free). ***E***, Summary of ACD (10 μM) or ethanol (EtOH, 21 mM) induced changes on firing rate recorded in the same mLHb neurons. ***F***, Summary of acetate (1 mM), EtOH (21 mM), or 4-MP (0.5 mM) +EtOH (21 mM) induced changes on firing rate recorded in mLHb neurons; $\&p < 0.05$ versus baseline; $^{a}p < 0.05$ EtOH versus 4-MP+EtOH. ***G***, Summary of DS (10 μM), ACD, or DS+ACD elicited potentiation on firing rate recorded in the same mLHb neurons; $\&\&p < 0.01$ versus baseline; $^{a}p < 0.05$ ACD versus DS+ACD. ***H1***, Mean time course of ACD-induced excitation in an mLHb neuron in the absence and presence of glutamate receptor antagonists (50 μM AP5 and 20 μM DNQX). ***H2***, The effect of ACD-induced increase in firing rate of mLHb neurons in the absence (ACD) and presence of AP5 and DNQX (AP5+DNQX+ACD); $^{\wedge}p < 0.05$, Student's paired *t* test.

endogenous aldehydes in the LHb. In the present of DS, ACD (10 μM) elicited a significantly greater acceleration of firing ($t_{(11)} = 2.5$, $p = 0.029$, ACD vs DS+ACD; Fig. 2*G*). This result suggests that the LHb is a target of DS, and therapeutics targeting the LHb may be beneficial for alcoholics.

ACD stimulates mLHb neurons involving glutamate receptors

LHb neurons are largely glutamatergic (Omelchenko et al., 2009; Meye et al., 2013) and receive strong glutamatergic inputs (Meye et al., 2013; Stamatakis et al., 2016; Yang et al., 2018). To

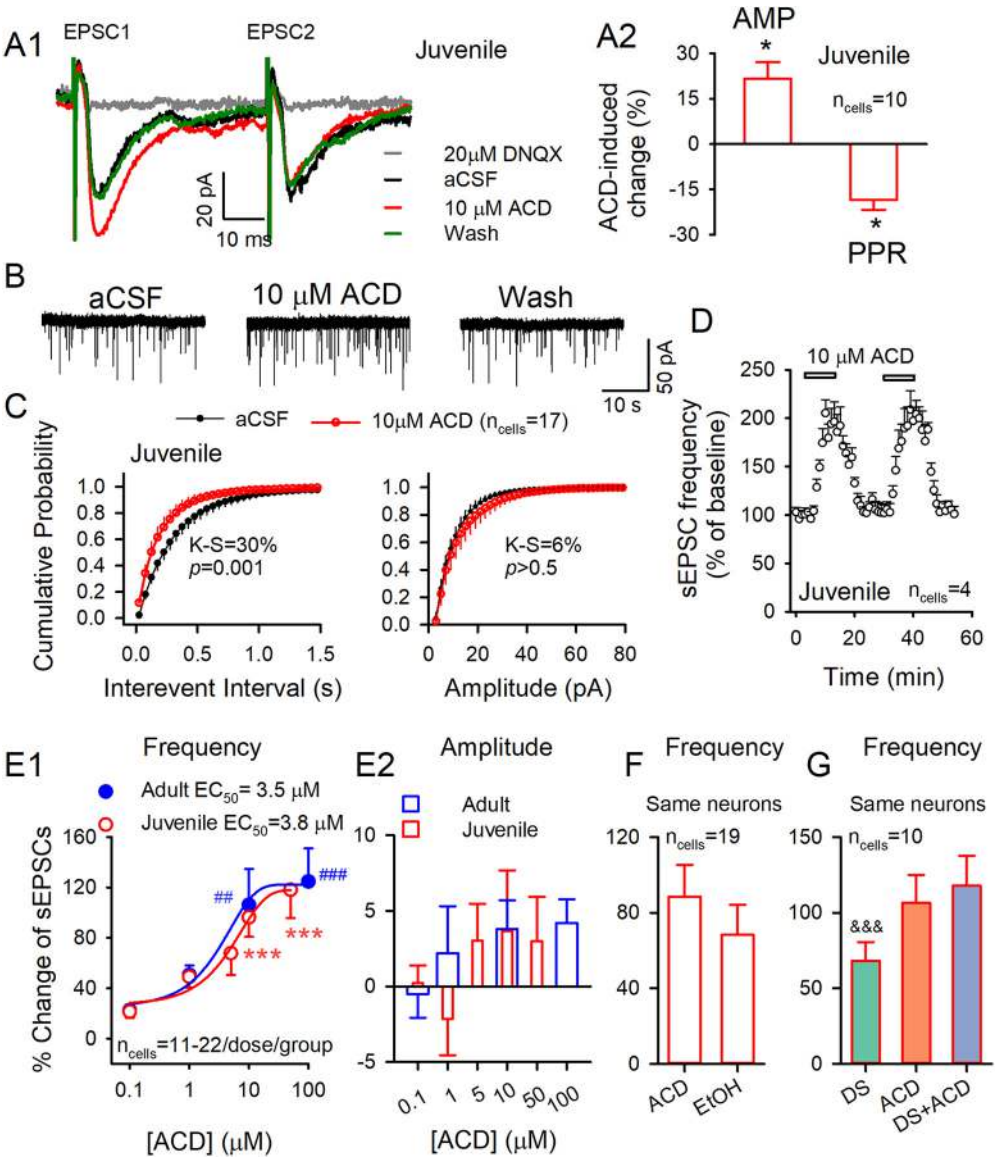

Figure 3. ACD facilitates glutamate release on mLHb neurons. The recording was performed at a holding potential of −60 mV in the presence of strychnine and gabazine. ***A1***, 10 μM ACD reversibly increased the amplitude of the first but not the second eEPSC induced by paired-pulse stimuli in the brain slices of the juvenile rats. ***A2***, Average % changes in eEPSC amplitude and PPR (PPR = $EPSC_2/EPSC_1$). ***B***, Current traces of sEPSCs obtained in the absence and the presence of 10 μM ACD. ***C***, ACD increased the average sEPSC frequency and cumulative probability of interevent intervals of sEPSCs but did not alter the cumulative probability of sEPSC amplitude in 17 neurons recorded. ***D***, Mean (±SEM) of the time course of change of sEPSC frequency induced by repeated application of 10 μM ACD from four mLHb neurons. ***E1***, Concentration-response relationship of the ACD-induced facilitation in sEPSC frequency. The curve was fitted with the logistic equation; $^{***}p < 0.001$ (juvenile); $^{\#\#}p < 0.01$, $^{\#\#\#}p < 0.001$ (adult); one-way ANOVA. ***E2***, ACD did not significantly alter the sEPSC amplitude. ***F***, Summary of changes induced by ACD (10 μM) or ethanol (EtOH, 21 mM) in sEPSCs recorded in the same mLHb neurons. ***G***, Summary of potentiation elicited by DS (10 μM), ACD, or DS+ACD on sEPSC frequency recorded in the same mLHb neurons (Student's paired *t* test, two-tails).

determine whether the ACD-induced acceleration of mLHb firing involves glutamatergic transmission, we compared the effect of ACD in the absence and the presence of AP5 (50 μM), and DNQX (20 μM), respectively, the NMDA, and AMPA/KA-type glutamate receptor antagonists, in the juvenile rats. The facilitation of firing induced by ACD was measured and reversed by washing. Then AP5 plus DNQX were applied to the brain slices for 8–10 min, followed by ACD reapplication. The application of these antagonists reduced the spontaneous firing by 27.0±8.2% ($t_{(4)} = 3.3$, $p = 0.011$ vs baseline), indicating that the LHb neurons are normally under the tonic control of glutamatergic transmission (Zuo et al., 2013; Gregor et al., 2019). In the presence of these antagonists, the increase in firing rate induced by ACD was significantly smaller than that in their absence ($t_{(4)} = 2.8$, $p = 0.048$; Fig. 2*H1*,*H2*).

ACD increases synaptic glutamate release in mLHb neurons

The above data indicate the involvement of glutamate receptors in ACD's facilitation of mLHb neuron firing; we next determined whether ACD would affect glutamatergic transmission in mLHb neurons. In the juvenile rats, under voltage clamp and at a holding potential (V_H) of −60 mV, EPSCs could be evoked by electrical stimulation applied by a local stimulating electrode. This current could be completely blocked by DNQX (Fig. 3*A1*, gray line), indicating that it is mediated by AMPA receptors. ACD (10 μM) reversibly enhanced the amplitude of the EPSCs in response to the first stimuli of the paired stimuli ($t_{(9)} = 3.6$, $p < 0.05$), but had no significant effect on the second one, and therefore decreased the pared-pulse ratio (PPR = $EPSC_2/EPSC_1$; $t_{(9)} = 3.9$, $p < 0.05$; Fig. 3*A1*,*A2*). Since a change in the PPR usually

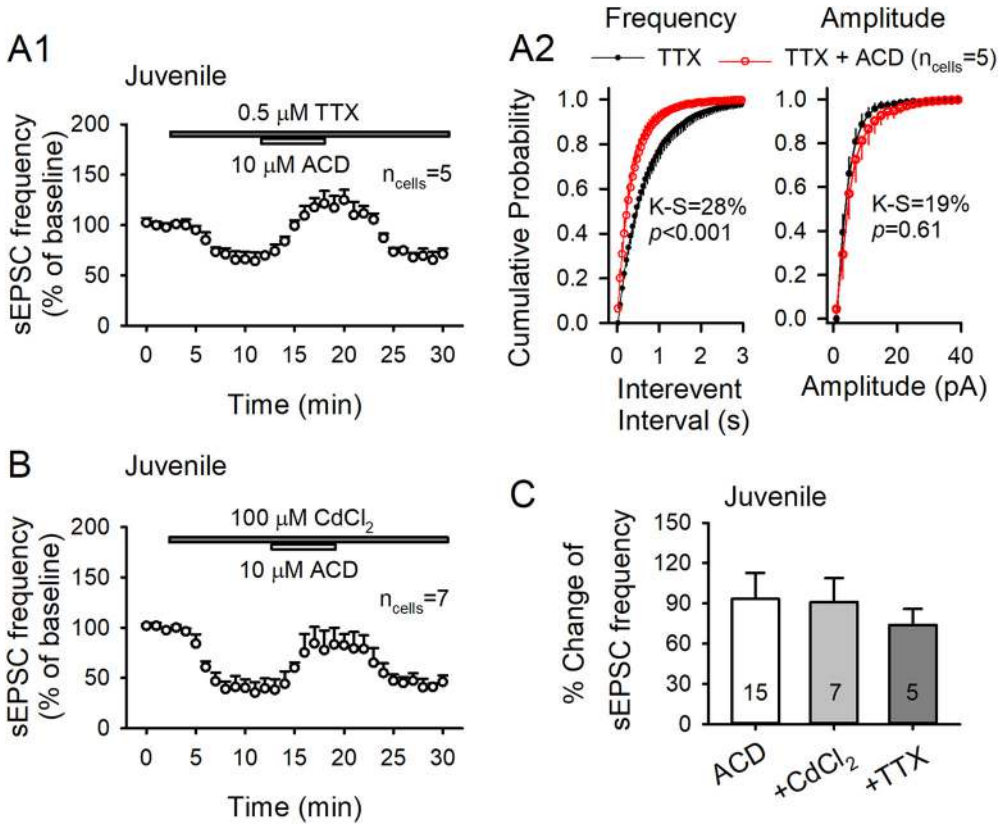

Figure 4. ACD's effect on sEPSCs is independent of TTX-sensitive sodium channels and voltage-gated calcium channels. ***A1***, Mean of the time courses of the ACD-induced increase in sEPSC frequency in the presence of TTX (***A1***) or $CdCl_2$ (***B***). ***A2***, The ACD-induced mean changes of the cumulative probability of interevent interval and amplitude in the presence of TTX. ***C***, Summary of % potentiation of sEPSC frequency induced by 10 μM ACD in aCSF and in the presence of $CdCl_2$ or TTX. One-way ANOVA.

indicates a presynaptic mechanism, these results suggest that ACD increases the probability of presynaptic glutamate release. This possibility is further supported by the following experiments, which show that ACD increases the frequency of the sEPSCs in the absence and presence of the voltage-gated sodium channel blocker TTX.

Bath application of ACD induced a significant, reversible, and reproducible increase of sEPSC frequency (Fig. 3*B*,*D*) in a concentration-dependent manner ($F_{(5,80)} = 10.4$, $p < 0.001$) with an EC_{50} of 3.8 μM ($r^2 = 0.98$; Fig. 3*E1*), but did not significantly change sEPSC amplitude ($F_{(5,80)} = 0.7$, $p = 0.61$; Fig. 3*E2*) in the juvenile rats. These results were confirmed by K-S tests (Fig. 3*C*). ACD also showed a similar effect on mLHb neurons in the adult rats ($F_{(4,84)} = 7.6$, $p < 0.001$), with an EC_{50} of 3.5 μM in sEPSC frequency ($r^2 = 0.97$; Fig. 3*E1*), without significant effect on sEPSC amplitude ($F_{(4,84)} = 1.0$, $p = 0.41$; Fig. 3*E2*). Bath application of ethanol (21 mM) caused an acceleration of sEPSC frequency like that by ACD (10 μM) in the same neurons (Fig. 3*F*). In addition, DS significantly increased sEPSC frequency ($t_{(9)} = 5.4$, $p < 0.001$ vs baseline). ACD tended to further potentiate glutamate release in the presence of DS ($t_{(9)} = 1.9$, $p = 0.09$, ACD vs DS+ ACD; Fig. 3*G*).

ACD-induced increase in sEPSCs in mLHb neurons is independent of sodium and calcium channels

A multitude of ion channels, including sodium and calcium channels on the presynaptic terminal, play a significant role in the process of transmitter release (Meir et al., 1999). We next determined whether ACD's effects on sEPSCs depend on sodium and calcium channels in the juvenile rats. The application of TTX (0.5 μM) significantly reduced the frequency and amplitude of sEPSCs, respectively, by 35.8 ± 7.3% ($t_{(4)} = 4.9$, $p < 0.01$) and 10.8 ± 2.6% ($t_{(4)} = 4.2$, $p < 0.001$), in keeping with our previous report (Zuo et al., 2013). However, the response to ACD (10 μM) persisted in the presence of TTX and was not significantly different from that seen in its absence ($F_{(2,24)} = 0.18$, $p = 0.84$; Fig. 4*A1*, *A2*,*C*). The application of $CdCl_2$ (100 μM), a non-selective voltage-gated calcium channel blocker, substantially reduced the frequency and amplitude of the sEPSCs (both $p < 0.05$; Fig. 4*B*). However, the response to ACD persisted in the presence of $CdCl_2$ and was not significantly different from that seen in its absence (Fig. 4*B*,*C*). These data show that ACD-induced increase in presynaptic glutamate release is independent of TTX sensitive sodium channels and voltage-gated calcium channels.

ACD-induced facilitation of firing and sEPSCs is mediated by DA D1 and D2 receptors

The LHb is subject to DA regulation. LHb neurons not only send projections (indirectly and directly) to midbrain DA neurons but also receive DA innervations (Shen et al., 2012; Hu et al., 2020). DA receptors (DARs) are present in the LHb and modulate the function of local cells (Good et al., 2013; Li et al., 2017). To determine whether ACD's action on mLHb neurons involves DARs, we compared ACD-induced facilitation of the spontaneous firings in the absence (aCSF) and presence of SCH23390 (10 μM) or raclopride (10 μM), respectively, D1R and D2R antagonists. In the juvenile rats, when applied alone, these antagonists did not significantly change the basal firing rate, in keeping with our previous report (Zuo et al., 2013). However, ACD acceleration of firings was substantially attenuated in SCH23390 ($t_{(5)} = 2.8$,

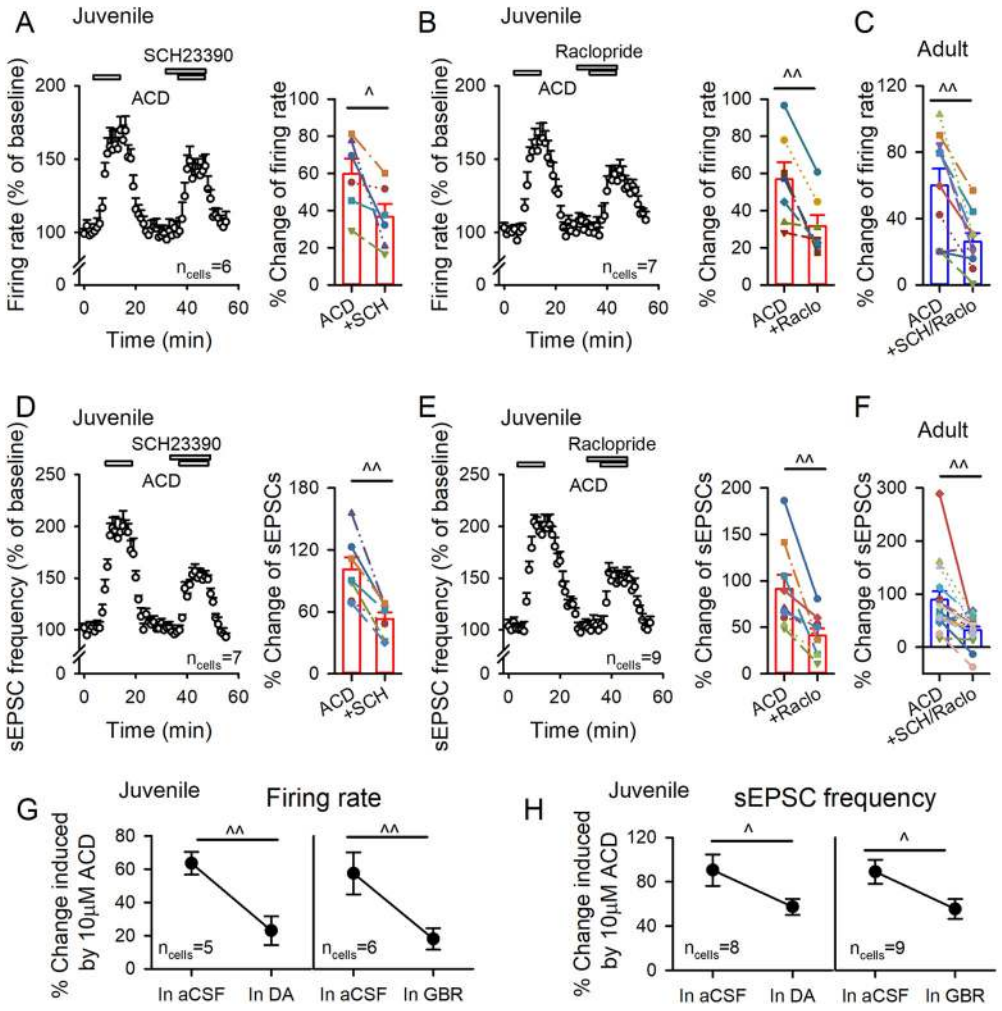

Figure 5. D1R antagonist SCH23390 and D2R antagonist raclopride attenuate ACD-induced increase in the frequency of firings and sEPSCs. Mean of the time courses of ACD's effect on the frequency of firing (***A***, ***B***, left panels) or sEPSCs (***D***, ***E***, left panels) from juvenile rats. ***A***, ***B***, ***D***, ***E***, right panels, Mean (±SEM) and individual values of ACD effects on the frequency of firings and of sEPSCs in the absence and presence of 10 μM SCH23390 or 10 μM raclopride from juvenile rats. Average and individual values of ACD effects on the frequency of firings (***C***) and of sEPSCs (***F***) in aCSF or SCH23390 plus raclopride from adult rats. Summary of ACD elicited potentiation on firing rate (***G***) and sEPSC frequency (***H***) in the absence and presence of DA (10 μM) or GBR (20 nM) recorded from juvenile rats; $^p < 0.05$, $^^p < 0.01$. Student's paired *t* test.

$p = 0.038$; Fig. 5*A*) or in raclopride ($t_{(6)} = 4.1$, $p = 0.006$; Fig. 5*B*). In the adult rats, in the presence of SCH23390 and raclopride, ACD-induced acceleration of firings was also substantially attenuated ($t_{(9)} = 4.5$, $p = 0.0015$; Fig. 5*C*).

To determine whether ACD's effect on glutamatergic transmission involves D1Rs and/or D2Rs, we compared the effects of ACD on sEPSC frequency in the absence and presence of SCH23390 or raclopride. In the juvenile rats, these antagonists did not significantly change the basal sEPSC frequency when they were applied alone. However, ACD-induced facilitation was substantially attenuated in SCH23390 ($t_{(6)} = 5.7$, $p = 0.0013$; Fig. 5*D*) or in raclopride ($t_{(8)} = 3.96$, $p = 0.004$; Fig. 5*E*). In the adult rats, ACD-induced acceleration of sEPSC frequency was also substantially attenuated ($t_{(15)} = 3.8$, $p = 0.0018$; Fig. 5*F*) in the presence of SCH23390 plus raclopride.

To test whether the ACD responses are attributed to an elevated dopaminergic activity, we pretreated slices with DA (10 μM) or the specific DA reuptake inhibitor GBR (20 nM) for 10 min before the co-application of ACD (10 μM). Notably, ACD-induced enhancement was significantly decreased after pretreating the LHb neurons with DA (firing: $t_{(4)} = 8.6$, $p = 0.0011$; sEPSCs: $t_{(7)} = 3.5$, $p = 0.011$) or GBR (firing: $t_{(5)} = 4.4$, $p = 0.007$; sEPSCs: $t_{(8)} = 2.81$, $p = 0.023$; Fig. 5*G*,*H*). These results support the view that ACD may increase DA levels, at least in part through decreasing DA reuptake.

ACD induces an inward current (I_{ACD}) by enhancing I_h activation

The above data indicate the presynaptic mechanisms involved in ACD's excitation of LHb neurons. To determine the possible postsynaptic mechanisms involved, we conducted the following experiments. As shown in Figure 6*A*, at a V_H of −60 mV and in the presence of TTX, strychnine, gabazine, DNQX, and AP5, which, respectively, block voltage-gated sodium channels, glycine, $GABA_A$, NMDA, and AMPA receptors, bath application of ACD induced a depolarizing inward current (I_{ACD}), in 57/72 (79.2%) cells tested in the juvenile rats. The peak value of I_{ACD} increased with the concentrations of ACD ($F_{(5,58)} = 15.7$, $p < 0.001$). By fitting the concentration-response curve to the Logistic function, we obtained an apparent EC_{50} of 5.3 μM ($r^2 = 0.97$; Fig. 6*B*), close to the EC_{50} (8.0 μM) for ACD facilitation of

LHb firing. I_{ACD} returned to the baseline level on washing, the peak amplitude induced by reapplication of ACD was not significantly different from that produced by the first application (Fig. 6*C*). I_{ACD} was also recorded on mLHb neurons in the adult rats, in a concentration-dependent manner ($F_{(4,40)} = 8.9$, $p < 0.001$), with an EC_{50} of 1.2 μM ($r^2 = 0.99$; Fig. 6*B*).

Hyperpolarization-activated and cyclic nucleotide-gated (HCN) channels are found in many neurons in the CNS, including the mLHb (Notomi and Shigemoto, 2004; Good et al., 2013; Simmons et al., 2020). To determine the potential role of HCN channels in I_{ACD}, I_{ACD} was measured and reversed by washing. Then, 20 μM ZD7288, an HCN channel blocker was applied to the brain slices for 8–10 min, followed by ACD reapplication. I_{ACD} was substantially attenuated in the presence of ZD7288 in LHb neurons of the juvenile rats ($t_{(8)} = 3.8$, $p = 0.005$; Fig. 6*C*,*D*) and adult rats ($t_{(7)} = 8.1$, $p < 0.001$).

To further examine the property of I_{ACD}, we next activated a family of hyperpolarized-activated current (I_h) using a series of hyperpolarizing voltage steps (Fig. 6*E1*). These currents were enhanced by ACD (10 μM), but reduced by ZD7288, suggesting that ACD activates HCN channels at this voltage range (Fig. 6*E1*). The plot of the peak values of I_h against the membrane voltage indicates that ACD induced a substantial increase in the ZD7288-sensitive I_h, from -68.6 ± 9.1 to -114.1 ± 14.4 pA at -120 mV ($t_{(5)} = 2.7$, $p < 0.05$; Fig. 6*E2*). Boltzmann functions fit to the plot of the normalized I_h peak values against membrane voltage indicates a significant depolarizing shift in half-activation voltage ($V_{1/2}$) from -99.9 ± 1.3 mV (in aCSF) to -93.1 ± 1.4 mV (in ACD; extra-sum-of-squares F test, $F_{(1,11)} = 25.9$, $p < 0.05$; Fig. 6*E3*). To isolate the I_h component that contributes to the total membrane currents activated by voltage steps, we deducted the currents recorded in the presence of ZD7288 from those recorded in normal aCSF, or from those recorded during the peak I_{ACD}. Using this method, we obtained the ZD7288-sensitive I_h component of the response that was present under aCSF and ACD conditions (Fig. 6*F*).

To determine the potential role of D1Rs and/or D2Rs in I_{ACD}, we compared I_{ACD} in the absence and presence of SCH23390 and raclopride. In the juvenile rats, neither SCH23390 ($n = 8$, $p > 0.05$) nor raclopride ($n = 7$, $p > 0.05$) had a significant effect on I_{ACD}. In the adult rats, however, the I_{ACD} was significantly attenuated ($t_{(7)} = 8.1$, $p < 0.001$; Fig. 6*D*) in the presence of SCH23390 plus raclopride.

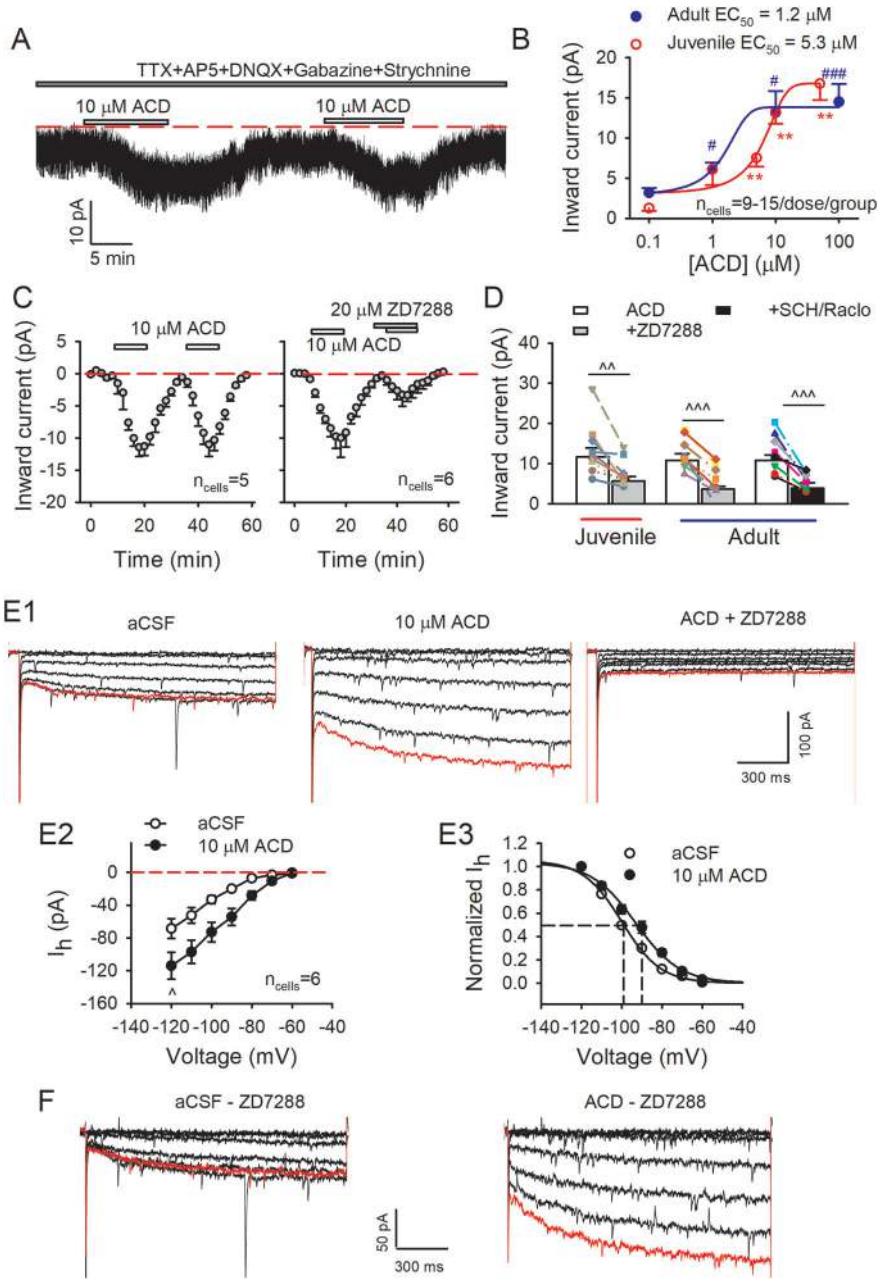

Figure 6. ACD enhances hyperpolarization-activated cation current in mLHb neurons. ***A***, A current trace of ACD-induced inward current in an mLHb neuron. ***B***, Concentration-response relationship of the inward current induced by ACD; $^{**}p < 0.01$ (juvenile); #$p < 0.05$, ###$p < 0.001$ (adult), one-way ANOVA. ***C***, Mean of the time course of inward current induced by ACD in the absence and presence of HCN channel blocker ZD7288. ***D***, Average and individual effects of ZD7288 or SCH23390 and raclopride on ACD-induced inward current; $^{\wedge\wedge}p < 0.01$, $^{\wedge\wedge\wedge}p < 0.001$, Student's paired t test. ***E1***, Current traces from an mLHb neuron in which 1.5 s, 10-mV hyperpolarizing pulses were applied from a holding potential of -60 mV to activate I_h. Pulses were applied during the peak of the current induced by ACD, and again during the peak of ZD7288 inhibition. ***E2***, The mean I-V relationship demonstrates that ACD enhances I_h is dependent on the voltage. We measured the peak values of the current during the last 50 ms of each voltage step. ***E3***, The normalized peak amplitude of I_h obtained during the control period and the peak effect of ACD were plotted against membrane potentials. Boltzmann functions were fit to the data points for the aCSF (○) and in the presence of 10 μM ACD (●). The data indicate that ACD induced a significant shift in the $V_{1/2}$. ***F***, Typical traces of I_h obtained by deducting currents recorded in the presence of ZD7288 from those recorded in the aCSF (ZD7288, left panel) or during the peak of ACD-induced current (ZD7288, right panel). This isolated I_h displays an enhanced I_h when ACD was applied.

ZD7288 attenuates ACD-induced facilitation on firing and sEPSC in mLHb neurons

To determine the potential role of HCN channels in the effects of ACD on firing and sEPSC in mLHb neurons, we compared the effect of ACD in the absence and presence of ZD7288. In the

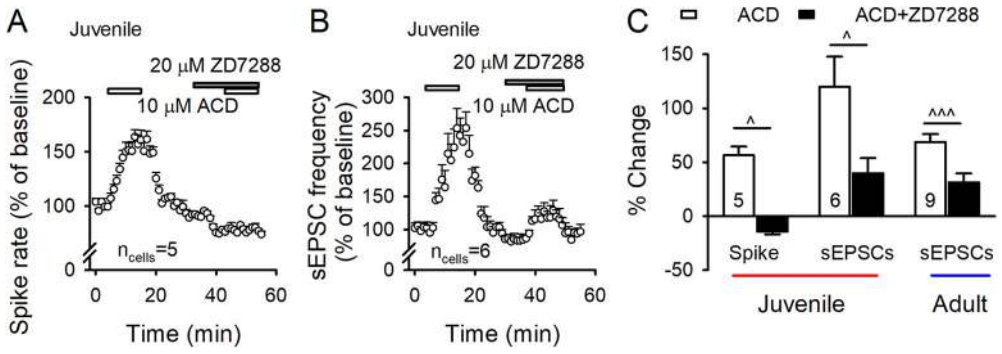

Figure 7. ZD7288 attenuates ACD-induced increase in the frequency of firing and of sEPSCs. Mean of the time course of ACD-induced increase the frequency of firing (***A***) and of sEPSCs (***B***) in the absence and presence of ZD7288. ***C***, Summary of ACD-induced change on firing and sEPSC frequency in the absence (ACD) and the presence of ZD7288 (ACD+ZD7288); $^{p} < 0.05$, $^{^}p < 0.01$, Student's paired *t* test.

juvenile rats, ZD7288 slightly but significantly reduced the firing rate (to 91.3 ± 2.1% of mean baseline frequency, $t_{(5)} = 4.12$, $p < 0.05$) and sEPSC frequency (to 84.8 ± 5.3%, $t_{(4)} = 2.88$, $p < 0.05$). Importantly, ZD7288 did not significantly alter sEPSC amplitude (to 99.0 ± 2.2%, $t_{(4)} = 0.43$, $p = 0.69$). These data indicate that the activity of mLHb neurons and the presynaptic glutamate release to mLHb neurons are normally under the tonic activation of HCN channels. In the presence of ZD7288, ACD-induced increase of firing was eliminated or even reversed, from 56.5 ± 8.1% in aCSF to −14.1 ± 2.6% in ZD7288 ($t_{(4)} = 3.9$, $p < 0.05$, Fig. 7*A*). Similarly, ACD-induced facilitation of sEPSC frequency was substantially attenuated in the presence of ZD7288 from juvenile ($t_{(5)} = 3.1$, $p < 0.05$; Fig. 7*B*,*C*) and adult rats ($t_{(8)} = 5.1$, $p < 0.001$; Fig. 7*C*). Remarkably, ZD7288 did not change sEPSC amplitude in the presence of ACD from either juvenile or adult rats (both $p > 0.5$). Based on this observation, we speculate that the HCN channels are present on the glutamatergic terminals targeting the LHb neurons.

cAMP-dependent PKA mediates ACD-induced facilitation of glutamate transmission and inward current on mLHb neurons

The cAMP-PKA signaling pathway has been implicated in the modulation of several ethanol-related behaviors (Wand et al., 2001; Ron and Messing, 2013), and ACD is known to mediate ethanol-induced PKA activation in the brain (Tarragon et al., 2014). Furthermore, there is previous evidence that cyclic nucleotides can act directly on HCN channels to shift their activation curve to more depolarized potentials (Wainger et al., 2001; Wang et al., 2020), and direct activation of adenylyl cyclase by bath application of forskolin induced an inward current in mLHb neurons, and increased sEPSC frequency in the LHb (Li et al., 2017). To determine the potential role of cAMP-PKA signaling in ACD's effects on mLHb neurons, we compared ACD's effects in the absence and presence of selective PKA antagonists Rp-cAMPs or KT-5720 in juvenile rats. Bath perfusion of Rp-cAMPs or KT-5720 (both are 10 μM for 6–8 min) slightly but significantly decreased sEPSC frequency, respectively, to 87.0 ± 2.0% ($t_{(6)} = 2.7$, $p < 0.05$) and to 92.2 ± 3.2% ($t_{(7)} = 2.4$, $p < 0.05$). These results show that the glutamatergic transmission in the LHb is normally under tonic PKA activation.

In the presence of Rp-cAMPs ($t_{(6)} = 5.4$, $p = 0.002$; Fig. 8*A*) or KT-5720 ($t_{(5)} = 3.6$, $p = 0.016$; Fig. 8*B*), ACD (10 μM)-induced facilitation of sEPSC frequency was substantially reduced. These results show that ACD-induced facilitation of glutamate transmission involves cAMP-PKA signaling. To determine the potential role of cyclic nucleotides in I_{ACD}, we compared the I_{ACD} recorded in the absence and presence of 10 μM Rp-cAMPs in the pipette solution for whole-cell recordings. We found that the peak amplitude of I_{ACD} induced by ACD was significantly reduced under this experimental condition ($t_{(17)} = 3.0$, $p = 0.008$; Fig. 8*C*).

Discussion

The central finding of this study is that ACD stimulated a subgroup of LHb neurons. The LHb hosts primarily glutamatergic neurons (Aizawa et al., 2012), but inhibits the brain's reward centers, including the dopaminergic ventral tegmental area (VTA) and the serotonergic dorsal raphe nucleus (DRN; Matsumoto and Hikosaka, 2007). Thus, LHb excitation might dampen the activity of serotoninergic and dopaminergic neurons. This effect of ACD may contribute to its aversive properties.

ACD excitation of LHb neurons

We first showed that ACD excited mLHb neurons, as reflected by the enhanced cFos expression after ACD administration at 100 and 300 mg/kg (intraperitoneal), doses that have been shown to induce CTA in rats (Correa et al., 2012), suggesting that ACD-induced CTA might be associated with mLHb neuron excitation. CTA induced by systemic administration of ACD may reflect a toxic aversive reaction (Brown et al., 1978; Aragon et al., 1991; Escarabajal et al., 2003). In support of this idea is the evidence that ACD was found in the CNS after systemic administration (Ward et al., 1997; Quertemont, 2004).

ACD excitation of LHb neurons through potentiation of glutamate synaptic transmission

Our electrophysiological data supports *in vivo* immunohistochemistry data. ACD increases the firing rate and the probability of synaptic glutamate release and induces an inward current in mLHb neurons. ACD's effect is quite potent: the EC_{50} is 8.0 μM in juvenile rats and 3.2 μM in adult rats for firing and 3.8 μM in juvenile rats and 3.5 μM in adult rats for sEPSC frequency. Notably, previous study has shown that after intragastrical administration of ethanol (4.5 g/kg) to rats ACD levels could reach 5–20 μM in brain interstitial fluid samples (Westcott et al., 1980). Moreover, cerebral blood ACD concentrations remain at μM levels for 30 min after ACD administration (100 mg/kg, i.p.; Quintanilla and Tampier, 2003). These data show doses exciting mLHb neurons *in vitro* are matched to that used *in vivo*. DNQX and AP5 attenuated ACD-induced acceleration of LHb firing, showing ACD's action is partly mediated by glutamatergic transmission. This is supported by evidence that ACD increased the

frequency but not amplitude of sEPSCs/mEPSCs and enhanced the amplitude of evoked EPSCs but reduced PPR. These results show ACD acts on the presynaptic site, increasing the probability of synaptic glutamate release. However, ACD's action on mLHb firing was not completely abolished by DNQX and AP5, suggesting other mechanisms may be involved.

ACD excitation of LHb neurons involves DA D1R and D2R activation

ACD excitation of mLHb neurons is mediated partly by DA D1 and D2 receptors. The DA system is known to contribute to ACD's pharmacological properties. ACD can excite VTA DA neurons (Foddai et al., 2004), increase DA release in target areas (Melis et al., 2007; Enrico et al., 2009; Deehan et al., 2013b), and promote cFos expression in DA terminal areas (Segovia et al., 2013). Conversely, DA transmission is found in the LHb. LHb neurons receive dopaminergic innervation from several brain regions, including the VTA (Brown and Shepard, 2013; Taylor et al., 2014). Limited enzymes in DA synthesis and DARs are found in the mLHb (Mansour et al., 1990; Bouthenet et al., 1991; Meador-Woodruff et al., 1991; Weiner et al., 1991; Aizawa et al., 2012; Jhou et al., 2013). In this study, the D1R antagonist SCH23390 attenuated ACD's acceleration of firing and EPSCs of mLHb neurons, showing the involvement of D1Rs. Intriguingly, D2R antagonist raclopride also reduced ACD-induced facilitation of firing and glutamatergic transmission in mLHb neurons, suggesting that ACD-induced excitation of mLHb neurons involves D2R activation. Besides, it also showed a similar effect was seen when SCH23390 was co-applied with raclopride. Data are consistent with a recent rodent study showing ACD operant drinking behavior involved D2R signaling (Brancato et al., 2014). Notably, recent studies found DA induced hyperpolarization in 25% of the mLHb neurons (Good et al., 2013), mediated by D2Rs (Jhou et al., 2013). These conflict with our data showing that D2R antagonist reduced ACD-induced increase in firing. The mechanisms underlying D2R activating neuronal excitability are unclear but may be independent of G_i (Yanovsky et al., 2011).

Unlike effects on firing and sEPSCs, D1R and D2R antagonists only attenuate I_{ACD} in the adult but not in juvenile mLHb neurons. Data from juvenile rats are consistent with a previous study showing that D1Rs and D2Rs are not involved in direct activation of mLHb neurons in postnatal (P15–P40) rats (Good et al., 2013). While the mechanisms underlying the apparent difference in the data between juveniles and adults are unclear, one interpretation is that D2R function changes during development (Meng et al., 1999; Labouesse et al., 2018).

ACD activation of LHb neurons through enhancing I_h and HCN channels

ACD induces a depolarizing I_{ACD} on ~80% of mLHb neurons, showing that ACD excitation of mLHb neurons also involves postsynaptic mechanisms. The HCN channel is a known target of ethanol in DA neurons (Okamoto et al., 2006; Rivera-Meza et al., 2014). As a pacemaker, HCN channels play a crucial role in regulating resting membrane potential and synaptic transmissions in many brain areas, including LHb (Wahl-Schott and Biel, 2009; Good et al., 2013). In the present study, ACD increased I_h. ZD7288, an HCN channel blocker, attenuated all actions of ACD on mLHb neurons, including firing, sEPSCs, and inward current. Results indicate ACD targets the HCN channel in mLHb neurons, which are probably present on the glutamatergic afferents to mLHb neurons, in addition to the dendrites of mLHb neurons (Poller et al., 2011).

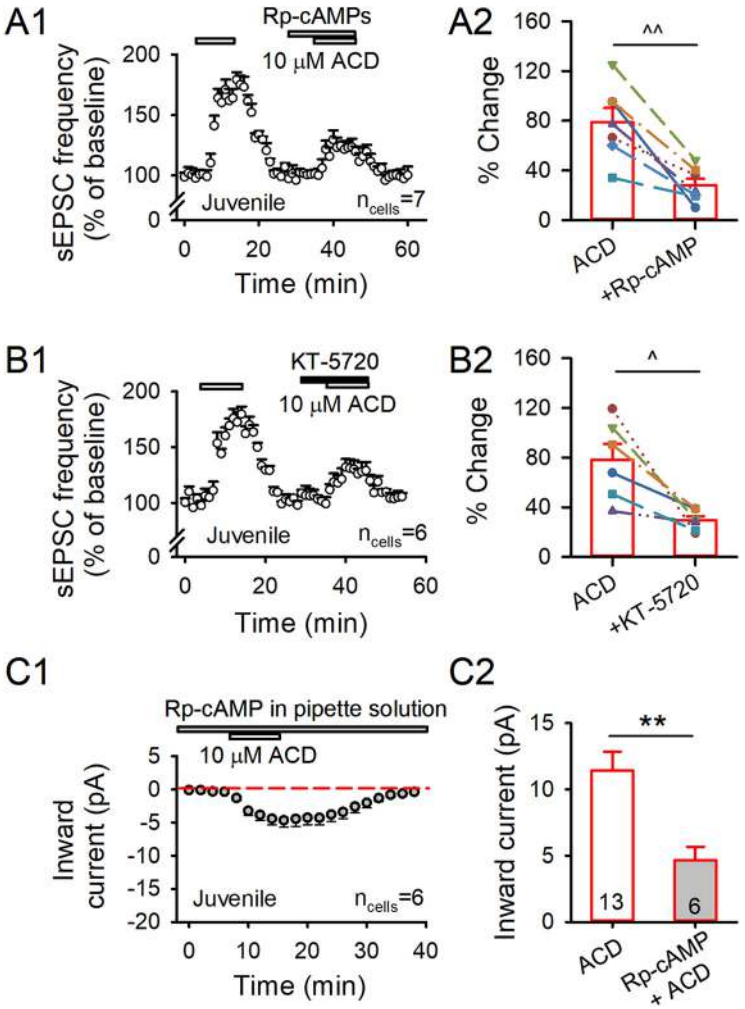

Figure 8. PKA antagonists attenuate the actions of ACD in mLHb neurons. Mean of the time courses of ACD's effect on sEPSC frequency in the presence of 10 μM Rp-cAMPs (***A1***) and 10 μM KT-5720 (***B1***) from juvenile rats. Mean and individual effects of ACD on sEPSC frequency in the presence Rp-cAMPs (***A2***) or KT-5720 (***B2***); $^p < 0.05$, $^{^}p < 0.01$, Student's paired *t* test. ***C1***, Mean of the time course of inward current induced by ACD in cells recorded with 10 μM Rp-cAMPs in the pipette solution. ***C2***, Summary of effects of ACD on inward current without (ACD) or with Rp-cAMPs in the pipette solution (Rp-cAMP + ACD); $^{**}p < 0.01$, Student's unpaired *t* test.

ACD excitation of LHb neurons involves cAMP-PKA signaling pathways

The PKA inhibitor Rp-cAMPs attenuated ACD-induced facilitation of sEPSCs and inward current. There is evidence that centrally formed ACD mediates ethanol-induced activation of PKA in the brain (Tarragon et al., 2014). Data in the present study suggest that ACD acts on mLHb neurons, activating cAMP-PKA-HCN signaling in the glutamatergic axons that project to mLHb neurons and in the somatodendrites of mLHb neurons.

Functional implication

The LHb is one of the few regions in the brain excited by aversive stimuli (Bromberg-Martin and Hikosaka, 2011). Addictive drugs, including cocaine and nicotine, have profound effects on LHb (Jhou et al., 2013; Zuo et al., 2013, 2016; Khaled et al., 2014; Glover et al., 2016). When the LHb is lesioned, voluntary ethanol intake of rodents is enhanced, indicating the LHb contributes to ethanol-induced aversion (Haack et al., 2014; Tandon et al., 2017). A limitation of the current study is that we did not identify the target area of ACD-activated mLHb neurons; however, we can speculate that RMTg and MRN might be the targets. Several lines of evidence supported this notion (Fu et al., 2017; Laurent et al., 2017; Fakhoury, 2018; Metzger et al., 2021). Although no direct evidence showing that ACD alters the extracellular DA and 5-HT levels in the mPFC, it has been reported that systemic administration of ACD (20 and 100 mg/kg) decreased the DA and 5-HT levels in the nucleus accumbens (Ward et al., 1997). These data indicate a negative reinforcement effect of ACD in the CNS.

ACD has been known as a strong aversive compound (Hunt, 1996; Quertemont et al., 2005). However, recent evidence suggests that ACD is aversive peripherally and rewarding centrally (Deehan et al., 2013a). Whereas systemic application of ACD induces CTA, intracerebral administration of ACD induces CPP, CTP, and self-administration (Peana et al., 2017). Electrophysiological studies demonstrated that ACD activates VTA dopaminergic neurons *in vivo* at doses up to 20 mg/kg (Enrico et al., 2009) and *in vitro* at concentrations up to 1000 nM (Diana et al., 2008), which is lower than was tested on mLHb neurons. Findings show that ACD's central rewarding property may be attributed to VTA dopaminergic neuron activation. However, this is inconsistent with current report showing that ACD activates the LHb, an "anti-reward" center, suggesting ACD has a central aversive property. It is arguable that ACD's central aversive effect may be shadowed by its rewarding effect and the net effect of ACD is revealed to be rewarding. Thus, the role of brain ACD might be more complex than previously thought.

In conclusion, the present study provides novel evidence on the potent excitatory effect of ACD on mLHb neurons via multiple cellular and molecular mechanisms. Although underlying mechanisms of how ACD activates LHb neurons have yet to be completely elucidated, our data suggest these effects are mediated partly by D1Rs and D2Rs that are most likely on glutamatergic afferents innervating LHb neurons. ACD excitation of LHb neurons is also involved in facilitating I_h and HCN channels and the cAMP-PKA signaling pathway. Given the importance of ACD in ethanol's actions, including aversion and the critical role of LHb neurons in conveying negative reward signals to midbrain dopaminergic neurons, we propose that ACD's actions on LHb neurons described here may be relevant to its central aversive properties.

References

Aizawa H, Kobayashi M, Tanaka S, Fukai T, Okamoto H (2012) Molecular characterization of the subnuclei in rat habenula. J Comp Neurol 520:4051–4066.

Aragon CM, Abitbol M, Amit Z (1991) Ethanol-induced CTA mediated by acetaldehyde through central catecholamine activity. Psychopharmacology (Berl) 103:74–77.

Barkley-Levenson AM, Cunningham CL, Smitasin PJ, Crabbe JC (2015) Rewarding and aversive effects of ethanol in high drinking in the dark selectively bred mice. Addict Biol 20:80–90.

Bouthenet ML, Souil E, Martres MP, Sokoloff P, Giros B, Schwartz JC (1991) Localization of dopamine D3 receptor mRNA in the rat brain using in situ hybridization histochemistry: comparison with dopamine D2 receptor mRNA. Brain Res 564:203–219.

Brancato A, Plescia F, Marino RA, Maniaci G, Navarra M, Cannizzaro C (2014) Involvement of dopamine D2 receptors in addictive-like behaviour for acetaldehyde. PLoS One 9:e99454.

Bromberg-Martin ES, Hikosaka O (2011) Lateral habenula neurons signal errors in the prediction of reward information. Nat Neurosci 14:1209–1216.

Brown PL, Shepard PD (2013) Lesions of the fasciculus retroflexus alter footshock-induced cFos expression in the mesopontine rostromedial tegmental area of rats. PLoS One 8:e60678.

Brown ZW, Amit Z, Smith B, Rockman GE (1978) Differential effects on conditioned taste aversion learning with peripherally and centrally administered acetaldehyde. Neuropharmacology 17:931–935.

Correa M, Salamone JD, Segovia KN, Pardo M, Longoni R, Spina L, Peana AT, Vinci S, Acquas E (2012) Piecing together the puzzle of acetaldehyde as a neuroactive agent. Neurosci Biobehav Rev 36:404–430.

Deehan GA Jr, Brodie MS, Rodd ZA (2013a) What is in that drink: the biological actions of ethanol, acetaldehyde, and salsolinol. Curr Top Behav Neurosci 13:163–184.

Deehan GA Jr, Engleman EA, Ding ZM, McBride WJ, Rodd ZA (2013b) Microinjections of acetaldehyde or salsolinol into the posterior ventral tegmental area increase dopamine release in the nucleus accumbens shell. Alcohol Clin Exp Res 37:722–729.

Diana M, Peana AT, Sirca D, Lintas A, Melis M, Enrico P (2008) Crucial role of acetaldehyde in alcohol activation of the mesolimbic dopamine system. Ann NY Acad Sci 1139:307–317.

Enrico P, Sirca D, Mereu M, Peana AT, Lintas A, Golosio A, Diana M (2009) Acetaldehyde sequestering prevents ethanol-induced stimulation of mesolimbic dopamine transmission. Drug Alcohol Depend 100:265–271.

Escarabajal MD, De Witte P, Quertemont E (2003) Role of acetaldehyde in ethanol-induced conditioned taste aversion in rats. Psychopharmacology (Berl) 167:130–136.

Fakhoury M (2018) The tail of the ventral tegmental area in behavioral processes and in the effect of psychostimulants and drugs of abuse. Prog Neuropsychopharmacol Biol Psychiatry 84:30–38.

Foddai M, Dosia G, Spiga S, Diana M (2004) Acetaldehyde increases dopaminergic neuronal activity in the VTA. Neuropsychopharmacology 29:530–536.

Fu R, Mei Q, Zuo W, Li J, Gregor D, Bekker A, Ye J (2017) Low-dose ethanol excites lateral habenula neurons projecting to VTA, RMTg, and raphe. Int J Physiol Pathophysiol Pharmacol 9:217–230.

Fu R, Tang Y, Li W, Ren Z, Li D, Zheng J, Zuo W, Chen X, Zuo QK, Tam KL, Zou Y, Bachmann T, Bekker A, Ye JH (2021) Endocannabinoid signaling in the lateral habenula regulates pain and alcohol consumption. Transl Psychiatry 11:220.

Gifuni AJ, Jozaghi S, Gauthier-Lamer AC, Boye SM (2012) Lesions of the lateral habenula dissociate the reward-enhancing and locomotor-stimulant effects of amphetamine. Neuropharmacology 63:945–957.

Glover EJ, McDougle MJ, Siegel GS, Jhou TC, Chandler LJ (2016) Role for the rostromedial tegmental nucleus in signaling the aversive properties of alcohol. Alcohol Clin Exp Res 40:1651–1661.

Good CH, Wang H, Chen YH, Mejias-Aponte CA, Hoffman AF, Lupica CR (2013) Dopamine D4 receptor excitation of lateral habenula neurons via multiple cellular mechanisms. J Neurosci 33:16853–16864.

Gregor DM, Zuo W, Fu R, Bekker A, Ye JH (2019) Elevation of transient receptor potential vanilloid 1 function in the lateral habenula mediates aversive behaviors in alcohol-withdrawn rats. Anesthesiology 130:592–608.

Haack AK, Sheth C, Schwager AL, Sinclair MS, Tandon S, Taha SA (2014) Lesions of the lateral habenula increase voluntary ethanol consumption and operant self-administration, block yohimbine-induced reinstatement of ethanol seeking, and attenuate ethanol-induced conditioned taste aversion. PLoS One 9:e92701.

Hu H, Cui Y, Yang Y (2020) Circuits and functions of the lateral habenula in health and in disease. Nat Rev Neurosci 21:277–295.

Hunt WA (1996) Role of acetaldehyde in the actions of ethanol on the brain–a review. Alcohol 13:147–151.

Jamal M, Ameno K, Tanaka N, Ito A, Takakura A, Kumihashi M, Kinoshita H (2016) Ethanol and acetaldehyde after intraperitoneal administration to Aldh2-knockout mice-reflection in blood and brain levels. Neurochem Res 41:1029–1034.

Jhou TC, Fields HL, Baxter MG, Saper CB, Holland PC (2009) The rostromedial tegmental nucleus (RMTg), a GABAergic afferent to midbrain dopamine neurons, encodes aversive stimuli and inhibits motor responses. Neuron 61:786–800.

Jhou TC, Good CH, Rowley CS, Xu SP, Wang H, Burnham NW, Hoffman AF, Lupica CR, Ikemoto S (2013) Cocaine drives aversive conditioning via delayed activation of dopamine-responsive habenular and midbrain pathways. J Neurosci 33:7501–7512.

Ji H, Shepard PD (2007) Lateral habenula stimulation inhibits rat midbrain dopamine neurons through a GABA(A) receptor-mediated mechanism. J Neurosci 27:6923–6930.

Kang S, Li J, Zuo W, Fu R, Gregor D, Krnjevic K, Bekker A, Ye JH (2017) Ethanol withdrawal drives anxiety-related behaviors by reducing M-type potassium channel activity in the lateral habenula. Neuropsychopharmacology 42:1813–1824.

Khaled MA, Pushparaj A, Di Ciano P, Diaz J, Le Foll B (2014) Dopamine D receptors in the basolateral amygdala and the lateral habenula modulate cue-induced reinstatement of nicotine seeking. Neuropsychopharmacology 39:3049–3058.

Labouesse MA, Sartori AM, Weinmann O, Simpson EH, Kellendonk C, Weber-Stadlbauer U (2018) Striatal dopamine 2 receptor upregulation during development predisposes to diet-induced obesity by reducing energy output in mice. Proc Natl Acad Sci USA 115:10493–10498.

Laurent V, Wong FL, Balleine BW (2017) The lateral habenula and its input to the rostromedial tegmental nucleus mediates outcome-specific conditioned inhibition. J Neurosci 37:10932–10942.

Li J, Zuo W, Fu R, Xie G, Kaur A, Bekker A, Ye JH (2016) High frequency electrical stimulation of lateral habenula reduces voluntary ethanol consumption in rats. Int J Neuropsychopharmacol 19:pyw050.

Li J, Kang S, Fu R, Wu L, Wu W, Liu H, Gregor D, Zuo W, Bekker A, Ye JH (2017) Inhibition of AMPA receptor and CaMKII activity in the lateral habenula reduces depressive-like behavior and alcohol intake in rats. Neuropharmacology 126:108–120.

Li W, Zuo W, Wu W, Zuo QK, Fu R, Wu L, Zhang H, Ndukwe M, Ye JH (2019) Activation of glycine receptors in the lateral habenula rescues anxiety- and depression-like behaviors associated with alcohol withdrawal and reduces alcohol intake in rats. Neuropharmacology 157:107688.

Mansour A, Meador-Woodruff JH, Bunzow JR, Civelli O, Akil H, Watson SJ (1990) Localization of dopamine D2 receptor mRNA and D1 and D2 receptor binding in the rat brain and pituitary: an in situ hybridization-receptor autoradiographic analysis. J Neurosci 10:2587–2600.

Mathis V, Kenny PJ (2019) From controlled to compulsive drug-taking: the role of the habenula in addiction. Neurosci Biobehav Rev 106:102–111.

Matsumoto M, Hikosaka O (2007) Lateral habenula as a source of negative reward signals in dopamine neurons. Nature 447:1111–1115.

Matsumoto M, Hikosaka O (2009) Two types of dopamine neuron distinctly convey positive and negative motivational signals. Nature 459:837–841.

Meador-Woodruff JH, Mansour A, Civelli O, Watson SJ (1991) Distribution of D2 dopamine receptor mRNA in the primate brain. Prog Neuropsychopharmacol Biol Psychiatry 15:885–893.

Meir A, Ginsburg S, Butkevich A, Kachalsky SG, Kaiserman I, Ahdut R, Demirgoren S, Rahamimoff R (1999) Ion channels in presynaptic nerve terminals and control of transmitter release. Physiol Rev 79:1019–1088.

Melis M, Enrico P, Peana AT, Diana M (2007) Acetaldehyde mediates alcohol activation of the mesolimbic dopamine system. Eur J Neurosci 26:2824–2833.

Meng SZ, Ozawa Y, Itoh M, Takashima S (1999) Developmental and age-related changes of dopamine transporter, and dopamine D1 and D2 receptors in human basal ganglia. Brain Res 843:136–144.

Metzger M, Souza R, Lima LB, Bueno D, Gonçalves L, Sego C, Donato J Jr, Shammah-Lagnado SJ (2021) Habenular connections with the dopaminergic and serotonergic system and their role in stress-related psychiatric disorders. Eur J Neurosci 53:65–88.

Meye FJ, Lecca S, Valentinova K, Mameli M (2013) Synaptic and cellular profile of neurons in the lateral habenula. Front Hum Neurosci 7:860.

Meye FJ, Soiza-Reilly M, Smit T, Diana MA, Schwarz MK, Mameli M (2016) Shifted pallidal co-release of GABA and glutamate in habenula drives cocaine withdrawal and relapse. Nat Neurosci 19:1019–1024.

Notomi T, Shigemoto R (2004) Immunohistochemical localization of Ih channel subunits, HCN1-4, in the rat brain. J Comp Neurol 471:241–276.

Okamoto T, Harnett MT, Morikawa H (2006) Hyperpolarization-activated cation current (Ih) is an ethanol target in midbrain dopamine neurons of mice. J Neurophysiol 95:619–626.

Omelchenko N, Bell R, Sesack SR (2009) Lateral habenula projections to dopamine and GABA neurons in the rat ventral tegmental area. Eur J Neurosci 30:1239–1250.

Peana AT, Sánchez-Catalán MJ, Hipólito L, Rosas M, Porru S, Bennardini F, Romualdi P, Caputi FF, Candeletti S, Polache A, Granero L, Acquas E (2017) Mystic acetaldehyde: the never-ending story on alcoholism. Front Behav Neurosci 11:81.

Poller WC, Bernard R, Derst C, Weiss T, Madai VI, Veh RW (2011) Lateral habenular neurons projecting to reward-processing monoaminergic nuclei express hyperpolarization-activated cyclic nucleotid-gated cation channels. Neuroscience 193:205–216.

Quertemont E (2004) Genetic polymorphism in ethanol metabolism: acetaldehyde contribution to alcohol abuse and alcoholism. Mol Psychiatry 9:570–581.

Quertemont E, Tambour S, Tirelli E (2005) The role of acetaldehyde in the neurobehavioral effects of ethanol: a comprehensive review of animal studies. Prog Neurobiol 75:247–274.

Quintanilla ME, Tampier L (2003) Brain mitochondrial aldehyde dehydrogenase: relation to acetaldehyde aversion in low-alcohol-drinking (UChA) and high-alcohol-drinking (UChB) rats. Addict Biol 8:387–397.

Rivera-Meza M, Quintanilla ME, Bustamante D, Delgado R, Buscaglia M, Herrera-Marschitz M (2014) Overexpression of hyperpolarization-activated cyclic nucleotide-gated channels into the ventral tegmental area increases the rewarding effects of ethanol in UChB drinking rats. Alcohol Clin Exp Res 38:911–920.

Rodd-Henricks ZA, Melendez RI, Zaffaroni A, Goldstein A, McBride WJ, Li TK (2002) The reinforcing effects of acetaldehyde in the posterior ventral tegmental area of alcohol-preferring rats. Pharmacol Biochem Behav 72:55–64.

Ron D, Messing RO (2013) Signaling pathways mediating alcohol effects. Curr Top Behav Neurosci 13:87–126.

Segovia KN, Vontell R, López-Cruz L, Salamone JD, Correa M (2013) c-Fos immunoreactivity in prefrontal, basal ganglia and limbic areas of the rat brain after central and peripheral administration of ethanol and its metabolite acetaldehyde. Front Behav Neurosci 7:48.

Shen X, Ruan X, Zhao H (2012) Stimulation of midbrain dopaminergic structures modifies firing rates of rat lateral habenula neurons. PLoS One 7: e34323.

Sheth C, Furlong TM, Keefe KA, Taha SA (2017) The lateral hypothalamus to lateral habenula projection, but not the ventral pallidum to lateral habenula projection, regulates voluntary ethanol consumption. Behav Brain Res 328:195–208.

Simmons SC, Shepard RD, Gouty S, Langlois LD, Flerlage WJ, Cox BM, Nugent FS (2020) Early life stress dysregulates kappa opioid receptor signaling within the lateral habenula. Neurobiol Stress 13:100267.

Stamatakis AM, Van Swieten M, Basiri ML, Blair GA, Kantak P, Stuber GD (2016) Lateral hypothalamic area glutamatergic neurons and their projections to the lateral habenula regulate feeding and reward. J Neurosci 36:302–311.

Tandon S, Keefe KA, Taha SA (2017) Excitation of lateral habenula neurons as a neural mechanism underlying ethanol-induced conditioned taste aversion. J Physiol 595:1393–1412.

Tarragon E, Baliño P, Aragon CMG (2014) Centrally formed acetaldehyde mediates ethanol-induced brain PKA activation. Neurosci Lett 580:68–73.

Taylor SR, Badurek S, Dileone RJ, Nashmi R, Minichiello L, Picciotto MR (2014) GABAergic and glutamatergic efferents of the mouse ventral tegmental area. J Comp Neurol 522:3308–3334.

Valentinova K, Tchenio A, Trusel M, Clerke JA, Lalive AL, Tzanoulinou S, Matera A, Moutkine I, Maroteaux L, Paolicelli RC, Volterra A, Bellone C, Mameli M (2019) Morphine withdrawal recruits lateral habenula cytokine signaling to reduce synaptic excitation and sociability. Nat Neurosci 22:1053–1056.

Wahl-Schott C, Biel M (2009) HCN channels: structure, cellular regulation and physiological function. Cell Mol Life Sci 66:470–494.

Wainger BJ, DeGennaro M, Santoro B, Siegelbaum SA, Tibbs GR (2001) Molecular mechanism of cAMP modulation of HCN pacemaker channels. Nature 411:805–810.

Wand G, Levine M, Zweifel L, Schwindinger W, Abel T (2001) The cAMP-protein kinase A signal transduction pathway modulates ethanol consumption and sedative effects of ethanol. J Neurosci 21:5297–5303.

Wang ZJ, Blanco I, Hayoz S, Brelidze TI (2020) The HCN domain is required for HCN channel cell-surface expression and couples voltage- and cAMP-dependent gating mechanisms. J Biol Chem 295:8164–8173.

Ward RJ, Colantuoni C, Dahchour A, Quertemont E, De Witte P (1997) Acetaldehyde-induced changes in monoamine and amino acid extracellular microdialysate content of the nucleus accumbens. Neuropharmacology 36:225–232.

Weiner DM, Levey AI, Sunahara RK, Niznik HB, O'Dowd BF, Seeman P, Brann MR (1991) D1 and D2 dopamine receptor mRNA in rat brain. Proc Natl Acad Sci USA 88:1859–1863.

Westcott JY, Weiner H, Shultz J, Myers RD (1980) In vivo acetaldehyde in the brain of the rat treated with ethanol. Biochem Pharmacol 29:411–417.

Yang Y, Wang H, Hu J, Hu H (2018) Lateral habenula in the pathophysiology of depression. Curr Opin Neurobiol 48:90–96.

Yanovsky Y, Li S, Klyuch BP, Yao Q, Blandina P, Passani MB, Lin JS, Haas HL, Sergeeva OA (2011) L-Dopa activates histaminergic neurons. J Physiol 589:1349–1366.

Ye JH, Zhang J, Xiao C, Kong JQ (2006) Patch-clamp studies in the CNS illustrate a simple new method for obtaining viable neurons in rat brain slices: glycerol replacement of NaCl protects CNS neurons. J Neurosci Methods 158:251–259.

Zhang F, Zhou W, Liu H, Zhu H, Tang S, Lai M, Yang G (2005) Increased c-Fos expression in the medial part of the lateral habenula during cue-evoked heroin-seeking in rats. Neurosci Lett 386:133–137.

Zimatkin SM (1991) Histochemical study of aldehyde dehydrogenase in the rat CNS. J Neurochem 56:1–11.

Zuo W, Chen L, Wang L, Ye JH (2013) Cocaine facilitates glutamatergic transmission and activates lateral habenular neurons. Neuropharmacology 70:180–189.

Zuo W, Xiao C, Gao M, Hopf FW, Krnjević K, McIntosh JM, Fu R, Wu J, Bekker A, Ye JH (2016) Nicotine regulates activity of lateral habenula neurons via presynaptic and postsynaptic mechanisms. Sci Rep 6:32937.

Zuo W, Fu R, Hopf FW, Xie G, Krnjević K, Li J, Ye JH (2017) Ethanol drives aversive conditioning through dopamine 1 receptor and glutamate receptor-mediated activation of lateral habenula neurons. Addict Biol 22:103–116.

Zuo W, Wu L, Mei Q, Zuo Q, Zhou Z, Fu R, Li W, Wu W, Matthew L, Ye JH (2019) Adaptation in 5-HT2 receptors-CaMKII signaling in lateral habenula underlies increased nociceptive-sensitivity in ethanol-withdrawn rats. Neuropharmacology 158:107747.